10

On PAPR Reduction Techniques in Mobile WiMAX

Imran Baig and Varun Jeoti
Universiti Teknologi PETRONAS, Malaysia

1. Introduction

The mobile Worldwide Interoperability for Microwave Access (Mobile WiMAX) air interface adopts orthogonal frequency division multiple access (OFDMA) as multiple access technique for its uplink (UL) and downlink (DL) to improve the multipath performance. All OFDMA based networks including mobile WiMAX experience the problem of high peak-to-average power ratio (PAPR). The literature is replete with a large number of PAPR reduction techniques. Among them, schemes like constellation shaping, phase optimization, nonlinear companding transforms, tone reservation (TR) and tone injection (TI), clipping and filtering, partial transmit sequence (PTS), precoding based techniques, selective mapping (SLM), precoding based selective mapping (PSLM) and phase modulation transform are popular. The precoding based techniques, however, show great promise as they are simple linear techniques to implement without the need of any complex optimizations. This chapter reviews these PAPR reduction techniques and presents a Zadoff-Chu matrix transform (ZCMT) based precoding technique for PAPR reduction in mobile WiMAX systems. The mobile WiMAX systems employing random-interleaved OFDMA uplink system has been used for determining the improvement in PAPR performance of the technique. It has been further used in selective mapping (SLM) based ZCMT precoded random-interleaved OFDMA uplink system. PAPR of these systems are analyzed with the root-raised-cosine (RRC) pulse shaping to keep out-of-band radiation low and to meet the transmission spectrum mask requirement. Simulation results show that the proposed systems have low PAPR than the Walsh-Hadamard transform (WHT) precoded random-interleaved OFDMA uplink systems and the conventional random-interleaved OFDMA uplink systems. The symbol-error-rate (SER) performance of these uplink systems is also better than the conventional random-interleaved OFDMA uplink systems and at par with WHT based random-interleaved OFDMA uplink systems. The good improvement in PAPR offered by the presented systems significantly reduces the cost and the complexity of the transmitter.

This chapter is organized as follows: Section 2 describes the background of the random-interleaved OFDMA uplink systems and SLM based random-interleaved OFDMA uplink systems, while in section 3, we present a detailed literature review. In section 4, we present our proposed system models with improved PAPR, section 5 presents the computer simulation results and section 6 concludes the chapter.

2. Background

The mobile Worldwide Interoperability for Microwave Access (Mobile WiMAX) is a broadband wireless solution that enables the convergence of mobile and fixed broadband networks through a common wide area radio-access (RA) technology and flexible network architecture. Since January 2007, the IEEE 802.16 Working Group (WG) has been developing a new amendment of the IEEE 802.16 standard i.e. IEEE 802.16m as an advanced air interface to meet the requirements of ITU-R/IMT-Advanced for 4G systems. The mobile WiMAX air interface adopts orthogonal frequency division multiple access (OFDMA) as multiple access technique for its uplink (UL) and downlink (DL) to improve the multipath performance. The scalable OFDMA (SOFDMA) is introduced in the IEEE 802.16e amendment to support scalable channel bandwidth.

OFDMA is a multiple access version of the orthogonal frequency division multiplexing (OFDM) systems. OFDMA system splits the high speed data stream into a number of parallel low data rate streams and these low rates data streams are transmitted simultaneously over a number of orthogonal subcarriers. The key difference between OFDM and OFDMA is that instead of being allocated all of the available subcarriers, the base station assigns a subset of carriers to each user in order to accommodate several transmissions at the same time. An inherent gain of the OFDMA based systems is its ability to exploit the multiuser diversity through subchannel allocation. Additionally, OFDMA has the advantage of simple decoding at the receiver side due to the absence of inter-carrier-interference (ICI). Other benefits of OFDMA include better granularity and improved link budget in the uplink communications (Knopp & Humblet, 1995; Tse, 1997).

There are two different approaches to do subcarrier mapping in OFDMA systems, localized subcarrier mapping and distributed subcarrier mapping. The distributed subcarrier mapping can be further divided in to two modes, interleaved mode and random interleaved mode. Fig.1 shows the subcarrier mapping in interleaved mode, where the subcarriers are mapped equidistant to each other's. Fig.2 explains the subcarrier mapping in random-interleaved mode, where the subcarriers are mapped randomly based on some permutation algorithm to each other's. Fig.3 further explains the concept of localized subcarrier mapping, where the subcarrier mapping is done in adjacent.

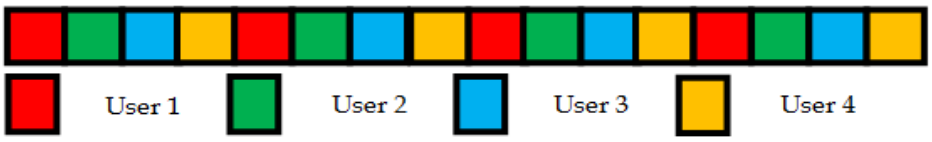

Fig. 1. Interleaved OFDMA

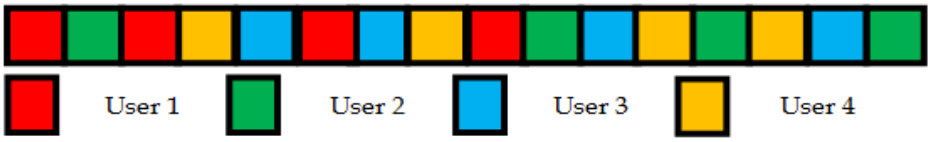

Fig. 2. Random-Interleaved OFDMA

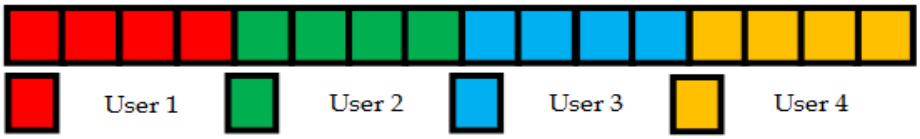

Fig. 3. Localized OFDMA

OFDMA is widely adopted in the various communication standards like WiMAX, mobile broadband wireless access (MBWA), evolved UMTS terrestrial radio access (E-UTRA) and ultra mobile broadband (UMB). OFDMA is also a strong candidate for the wireless regional area networks (WRAN) and the long term evaluation advanced (LTE-Advanced).

However, OFDMA has some drawbacks, among others; the peak-to-average power ratio (PAPR) is still one of the major drawbacks in the transmitted OFDMA signal (Wang & Chen, 2004). Therefore, for zero distortion of the OFDMA signal, the high-power-amplifier (HPA) must not only operate in its linear region but also with sufficient back-off. Thus, HPA with a large dynamic range is required for OFDMA systems. These amplifiers are very expensive and are major cost component of the OFDMA systems.

Thus, if we reduce the PAPR it not only means that we are reducing the cost of OFDMA systems and reducing the complexity of analog-to-digital (A/D) and digital-to-analog (D/A) converters, but also increasing the transmit power, thus, for same range improving received signal-noise-ratio (SNR), or for the same SNR improving range. Fig.4 illustrates the block diagram of the OFDMA uplink systems. In OFDMA uplink systems the baseband modulated symbols are passed through serial-to-parallel (S/P) converter which generates complex vector of size M. We can write the complex vector of size M as follows:-

$$X = [X_0, X_1, X_2 \ldots X_{M-1}]^T \tag{1}$$

Then the subcarrier mapping of these constellations symbols can be done on in one of the subcarrier mapping mode: interleaved mode, random-interleaved mode or in localized mode respectively. After the subcarrier mapping, we get frequency domain samples: $\{\hat{Y}_l : l = 0,1,2,\ldots,N-1\}$. Mathematically, the subcarrier mapping in interleaved mode can be done as follows:-

$$\hat{Y}_l = \begin{cases} X_{\frac{l}{Q}} & ,l = Q.k \quad 0 \le k \le M-1 \\ 0 & otherwise \end{cases} \tag{2}$$

where N : System subcarriers, M : User subcarriers, Q : Subchannels/Users, (Q=N/M), 0 ≤ l ≤ N-1 and N=Q.M. The subcarrier mapping in random-interleaved mode can be done mathematically as follows:-

$$\hat{Y}_l = \begin{cases} X_{\frac{l}{\hat{Q}}} & ,l = \hat{Q}.k \quad 0 \le k \le M-1 \\ 0 & otherwise \end{cases} \tag{3}$$

where, 0 ≤ l ≤ N-1 and N=Q.M, and $0 \le \hat{Q} \le Q$. The subcarrier mapping in localized mode can be done mathematically as follows:-

$$\hat{Y}_l = \begin{cases} X_l & 0 \le l \le M-1 \\ 0 & M \le l \le N-1 \end{cases} \quad (4)$$

The k^{th} subcarrier of each group is assigned to the k^{th} user with index set {(k), (Q+k), …, (((M-1) Q+k)}. Suppose the k^{th} user is assigned to subchannel k then the complex baseband ZCMT precoded interleaved OFDMA uplink signal for k^{th} user can be written as follows:-

$$x_n^{(k)} = \sum_{l=0}^{L-1} \hat{Y}_l^{(k)} . e^{j2\pi \frac{(lQ+k)}{N} n}, \; n = 0,1 \ldots N-1 \quad (5)$$

The k^{th} subcarrier of each group is assigned to the k^{th} user with index set: $\{(\gamma_{q,1}),(Q+\gamma_{q,2}),\ldots,(M-1)Q+\gamma_{q,M-1})\}$, where $\{(\gamma_{q,1}),(\gamma_{q,2}),\ldots,(\gamma_{q,M-1})\}$ are independent and identically distributed random variables with uniform distribution on (q=0,1,2,…,Q-1). Suppose the k^{th} user is assigned to sub-channel k then the complex baseband random-interleaved OFDMA signal for k^{th} user with N system subcarriers and M user subcarriers can be written as follows:-

$$x_n^{(k)} = \sum_{l=0}^{L-1} (\hat{Y}_l^{(k)} . e^{j2\pi \frac{(lQ+\gamma_{q,k})}{N} n}), \; n = 0,1 \ldots N-1 \quad (6)$$

The subchannel k is composed of subcarriers with index set {(kL), (kL+1), (kL+2)… (kL+L-1)}, where k=0,1,2,…, Q-1. Suppose the k^{th} user is assigned to subchannel k then the complex baseband ZCMT precoded localized OFDMA uplink signal for k^{th} user can be written as follows:-

$$x_n^{(k)} = \frac{1}{\sqrt{N}} \sum_{l=0}^{L-1} (\hat{Y}_l^{(k)} . e^{j2\pi \frac{(kL+l)}{N} n}), \; n = 0,1 \ldots N-1 \quad (7)$$

$\hat{Y}_l^{(k)}$ is modulated signal on subcarrier l for k^{th} user.

The complex passband signal of OFDMA uplink systems after the RRC pulse shaping can be written as follows:-

$$x(t) = e^{j\omega_c t} \sum_{n=0}^{N-1} x_n^{(k)} . r(t - n\breve{T}) \quad (8)$$

where, ω_c is carrier frequency, $r(t)$ is baseband pulse, $\breve{T} = (\frac{M}{N}).T$ is compressed symbol duration after IFFT and T is symbol duration is seconds. The RRC pulse shaping filter can be defined as follows:-

$$r(t) = \frac{sin\left(\frac{\pi t}{\breve{T}}(1-\alpha)\right) + 4\alpha \frac{t}{\breve{T}} cos\left(\frac{\pi t}{\breve{T}}(1+\alpha)\right)}{\frac{\pi t}{\breve{T}} \cdot \left(1 - \frac{16\alpha^2 t^2}{\breve{T}^2}\right)} \quad (9)$$

$0 \le \alpha \le 1$, where α is rolloff factor. The PAPR of OFDMA uplink signal in (8) with RRC pulse shaping can be written as follows:-

$$PAPR = \frac{\max\limits_{0 \le t \le N\breve{T}} |x(t)|^2}{\frac{1}{N\breve{T}} \int_0^{N\breve{T}} |x(t)|^2 dt} \quad (10)$$

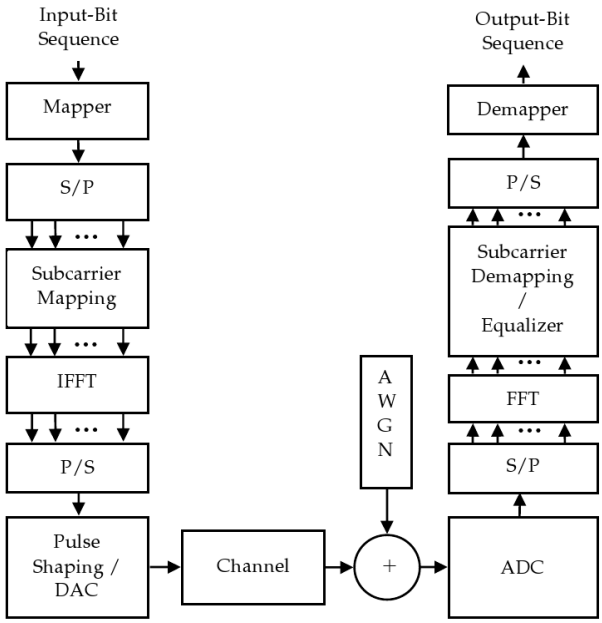

Fig. 4. Random-Interleaved OFDMA uplink system

3. Literature review

A large number of PAPR reduction techniques have been proposed in the literature. Among them, schemes like phase optimization (Nikookar & Lidsheim, 2002), constellation shaping (Kou et al., 2007), selective mapping (SLM) (Lim et al., 2005), nonlinear companding transforms (Jiang et al., 2006), tone reservation (TR), tone injection (TI) (Mourelo., 1999; Yoo et al., 2006), partial transmit sequence (PTS) (Han & Lee, 2004; Müller & Huber, 1997; Cimini & Sollenberger, 2000; Tellambura, 2001), clipping and filtering (Wang & Tellambura, 2005; Li & Cimini, 1998; Nee & Wild, 1998), precoding based techniques (Slimane, 2007; Min & Jeoti, 2007; Baig & Jeoti, 2010a, 2010b, 2010c), precoding based selective mapping (PSLM) techniques (Baig & Jeoti, 2010a, 2010b) and phase modulation transform (Tasi et al., 2006; Thompson et al., 2008) are popular. The precoding based techniques, however, show great promise as they are simple linear techniques to implement without the need of any side information. Additionally, the precoding based techniques take advantage of $\tilde{T} = (\frac{M}{N}).T$ frequency variations of the communication channel and offers substantial performance gain in fading multipath channels. In the following sub-section we focus more closely on the PAPR reduction techniques for multicarrier transmission.

3.1 Clipping and filtering techniques

The clipping techniques are simpler and commonly used to reduce the PAPR (Wang & Tellambura, 2005; Li & Cimini, 1998; Nee & Wild, 1998). These techniques apply clipping or

nonlinear saturation around the peaks to lower the high PAPR produced by the multicarrier transmitter. It is straightforward to clip the signal parts that are outside the tolerable area. Clipping techniques introduces in-band or out-of-band distortions that can destroy the orthogonality between the subcarriers. Generally, the clipping operation is carried out at the transmitter. On the other hand, the receiver requires to estimate the clipping that has been carried out at the transmitter and to compensate the received OFDM symbol accordingly. Normally, most of the time no more than one clipping happens per OFDM symbol. Hence, the receiver has to approximate the size and the location of the clip. However, it is hard to get related information. After the clipping operation, the filtering operation can noticeably decrease the out-of-band radiation.

Unfortunately, the in-band distortion cannot be reduced by the filtering operation. On the other hand, the clipping can introduce some peak re-growth. So, after the clipping operation and filtering operation the signal may exceed the clipping level at some points. To decrease the peak re-growth, a repeated clipping operation and filtering operation can be carried out to obtain a desirable PAPR at the expense of computational complexity increase. Fig.5 shows represent the clipped edition of the $x^p[m]$, which can be written as follows:-

$$x_c^p[m] = \begin{cases} -\mathrm{A} & x^p[m] \leq -A \\ x^p[m] & |x^p[m]| < A \\ \mathrm{A} & x^p[m] \geq A \end{cases} \tag{11}$$

or

$$x_c^p[m] = \begin{cases} x^p[m] & x^p[m] \leq -A \\ \frac{x^p[m]}{x^p[m]}.\mathrm{A} & \text{Otherwise} \end{cases} \tag{12}$$

where A is pre-determined clipping level. The equation (12) can be used for both baseband complex-valued signals and passband real-valued signals and the equation (11) can only be used for the passband signals only. The clipping-ratio (CR) normalized by the root-mean-square (RMS) value σ of OFDM signal can be written as follows:-

$$\mathrm{CR} = \mathrm{A}/\sigma \tag{13}$$

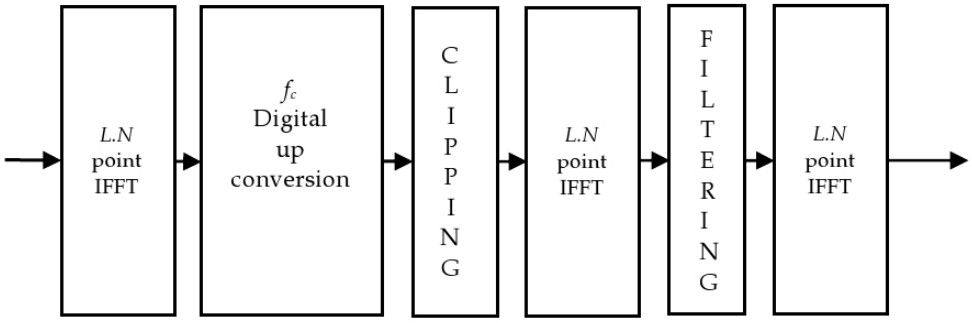

Fig. 5. Block Diagram of OFDM System with Clipping and Filtering (Cho et al., 2011)

3.2 Selective Mapping (SLM)

The SLM is one of the most popular PAPR reduction techniques in the literature (Lim et al., 2005). This technique is based on the phase rotations. In SLM based OFDM (SLM-OFDM) systems, a set of V different data blocks are created at the transmitter representing the identical information and a data block with minimum PAPR is selected for the transmission. Fig.6 shows the general block diagram of the SLM-OFDM system. Every data block is multiplied with the V dissimilar phase sequences, each of length N, $B^{(v)} = [b_{v,0}, b_{v,1}, \ldots, b_{v,N-1}]^T$, $v = 1, 2 \ldots V$, which results in the changed data blocks. Now suppose the altered data block for the v^{th} phase sequence is given by $X^{(v)} = [X_0 b_{v,0}, X_1 b_{v,1}, \ldots, X_{N-1} b_{v,N-1}]^T$, $v=1, 2 \ldots V$. Each X_n^v can be defined as follows:-

$$X_n^v = X_n b_{v,n} \quad , \quad (1 \le v \le V) \tag{14}$$

After applying SLM to X, the OFDM signal becomes as follows:-

$$x_n^{(v)} = \frac{1}{\sqrt{N}} \sum_{k=0}^{N-1} X_k^v . e^{j2\pi \frac{n}{N} k} \text{ , n=0, 1, 2... } N\text{-1} \tag{15}$$

where, $v = 1, 2 \ldots V$. Amongst all the tailored data blocks: $x^{(v)}$, $v = 1, 2 \ldots V$, the data block with minimum PAPR is selected for the transmission. Side information about the selected phase sequence must be communicated to the receiver which performs the reverse operation in order to recover the actual data block.

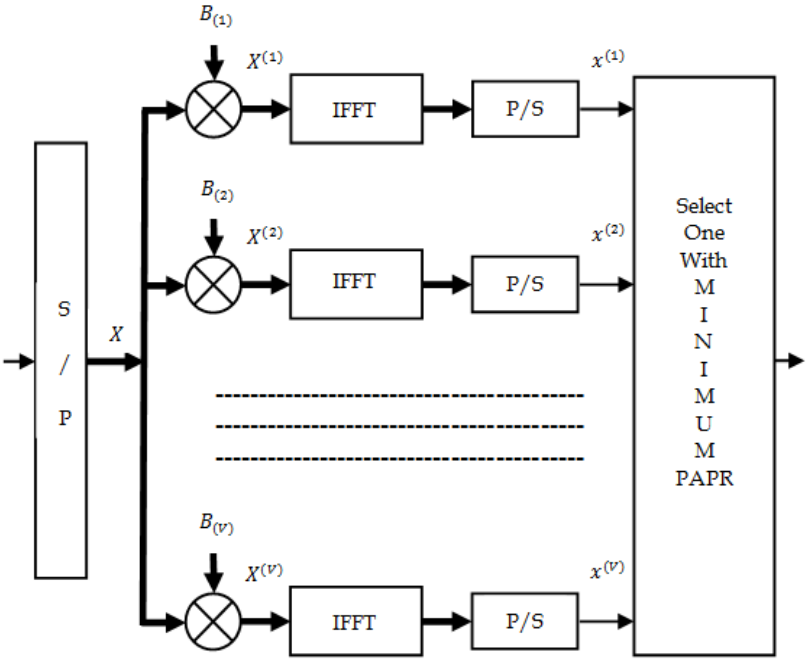

Fig. 6. Block diagram of OFDM system with Selective Mapping (Han & Lee, 2005)

3.3 Partial Transmit Sequence (PTS)

PTS is another very popular PAPR reduction technique (Han & Lee, 2004; Müller & Huber, 1997; Cimini & Sollenberger, 2000; Tellambura, 2001). In this technique, the input data block of N symbols is partitioned into disjoint sub-blocks. In each sub-block, the subcarriers are weighted by a phase factor. The phase factors are chosen in such a way so that the PAPR of the combined signal is reduced. Fig.7 shows the general block diagram of the PTS PAPR reduction technique. In the PTS technique input data block X is partitioned into M disjoint sub-blocks: $X^m = [X^{m,0}, X^{m,1}, \ldots, X^{m,N-1}]^T$, $m = 1,2,3,\ldots,M$, such that $\sum_{m=1}^{M} X^m = X$ and the sub-blocks are combined to reduce the PAPR in the time-domain. The L-times oversampled time-domain signal of X_m, $m=1,2,3,\ldots,M$ is denoted by: $x^m = [x^{m,0}, x^{m,1}, \ldots, x^{m,N-1}]^T$, $m=1,2,3,\ldots,M$ is obtained by obtained by taking an IFFT of length NL on X^m concatenated with $(L-1)N$ zeros. These are called PTS. Complex phase factors $b^m = \exp(j\Phi m)$, $m=1,2,3,\ldots M$, are launched to combine the PTSs. The set of phase factors is designated as a vector: $\hat{b} = [\hat{b}^1, \hat{b}^2, \ldots, \hat{b}^M]^T$. The time domain-signal after combining can be written as follows:-

$$x = \sum_{m=1}^{M} \hat{b}^m . x^m \tag{16}$$

The key idea is to find out the set of phase factors that reduces the PAPR. Generally, to reduce the search complexity, the selection of the phase factors is bounded by a set with a finite number of elements. The set of acceptable phase factors can be written as: $P = \{e^{j2\pi \frac{l}{W}} : l = 0,1,2,\ldots,W-1\}$, where W is the number of permitted phase factors. Additionally, we can set $b^1 = 1$ without any loss of the performance.

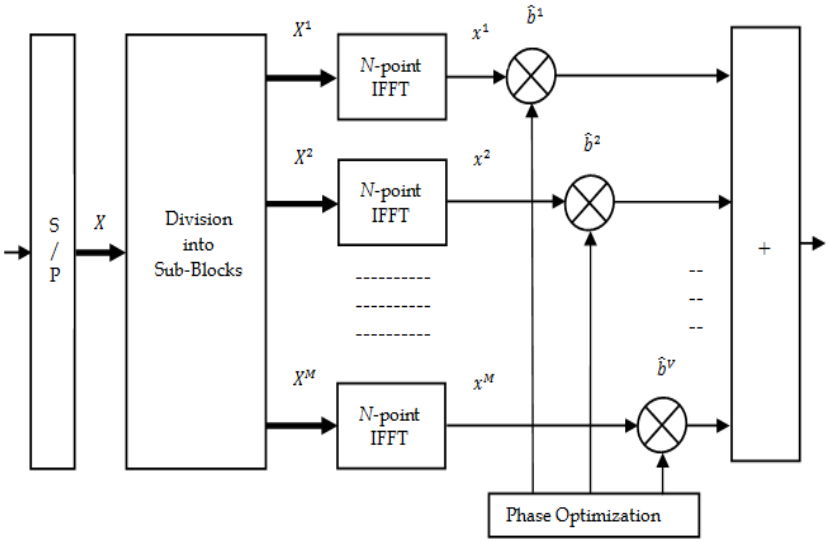

Fig. 7. Block diagram of OFDM system with Partial Transmit Sequence (Müller & Huber, 1997)

Therefore, we should execute a complete search for (M-1) phase factors. So, to find the optimum set of phase factors the W^{M-1} sets of phase factors are searched. If we increase the number of sub-blocks M, the search complexity is increases exponentially. PTS needs M IFFT operations for every data block, and the number of needed side information bits is $[\log_2 W^{M-1}]$. The amount of PAPR reduction is based on the number of sub-blocks M and the number of permitted phase factors W. Subblock partitioning is another factor that may have an effect on the PAPR gain PTS, which is the way of partition of the subcarriers into several disjoint sub-blocks. There are three kinds of sub-block partitioning techniques: interleaved, pseudo-random and adjacent partitioning.

Among them, pseudo-random partitioning has been found to be the best choice for PTS. The PTS technique can work with a random number of subcarriers and any modulation scheme. As mentioned above, the ordinary PTS technique has exponentially increasing search complexity. To lower the search complexity, a range of techniques have been proposed in the literature. Once the PAPR falls below a set threshold, the iterations for updating the set of phase factors must be stopped. Number of techniques has been presented in the literature to reduce the number of iterations. These techniques achieve considerable reduction in search complexity with minor PAPR performance degradation.

Example: The PTS PAPR reduction technique for an OFDM system can be explained with a simple example (Han & Lee, 2005). Here, we take eight subcarriers that are divided into four sub-blocks. The phase factors are selected in P ={±1}. Fig.8 illustrates the adjacent sub-block partitioning for a data block X of size 8. The original data block X has a PAPR of 6.5 dB. There are 8 ways to mix the sub-blocks with fixed b^1 =1.

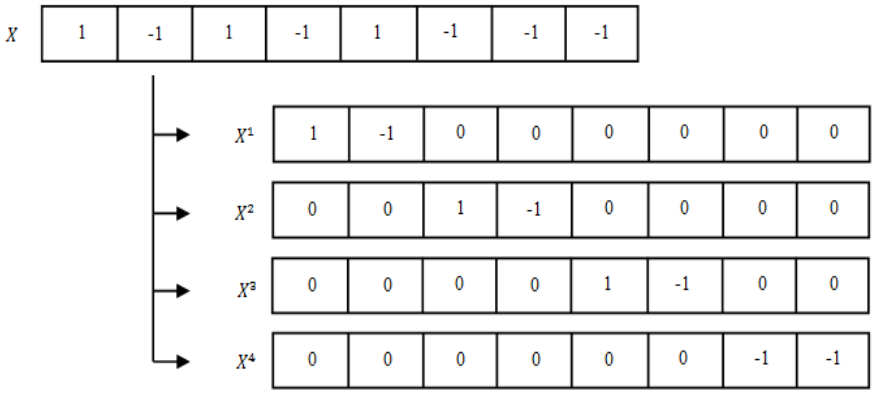

Fig. 8. An example of adjacent subblock partitioning in PTS (Han & Lee, 2005)

Amongst them $[\hat{b}^1, \hat{b}^2, \hat{b}^3, \hat{b}^4]^T = [1,-1,-1,-1]^T$ gets the lower PAPR. The tailored data block will be $X = \sum_{m=1}^{M} \hat{b}^m . X^m = [1,-1,-1,1,-1,1,1,1]$ whose PAPR is 2.2 dB, resulting in a 4.3 dB PAPR gain. In this case, the number of necessary IFFT operations is 4 and the amount of side information is 3 bits. The side information should be transmitted to the receiver for the recovery of original data block. There are many ways to transmit side information; one of

the ways is to transmit side information bits with a separate channel other than the data channel. Another ways is to include the side information within the data block but it results in data rate loss.

3.4 Precoding based techniques

Precoding based techniques are simple linear techniques. These techniques can reduce the PAPR up to the PAPR of single carrier systems (Slimane, 2007). Walsh-Hadamard transform (WHT) precoding based techniques, discrete cosine transform (DCT) precoding based techniques, discrete hartley transform (DHT) precoding based techniques are common examples of precoding based PAPR reduction techniques (Slimane, 2007; Min & Jeoti, 2007; Baig & Jeoti, 2010a, 2010b, 2010c).

3.4.1 Walsh-Hadamard Transform (WHT)

WHT is an orthogonal linear transform and can be implemented by a butterfly structure as in FFT. This means that applying WHT does not require the extensive increase of system complexity. The kernel of WHT can be written as follows:-

$$H_1 = [1] \tag{17}$$

$$H_2 = \frac{1}{\sqrt{2}}\begin{bmatrix} 1 & 1 \\ 1 & -1 \end{bmatrix} \tag{18}$$

$$H_{2N} = \frac{1}{\sqrt{2N}}\begin{bmatrix} H_N & H_N \\ H_N & H_N^{-1} \end{bmatrix} \tag{19}$$

where H_N^{-1} denotes the binary complement of H^N.

3.4.2 Discrete Hartley Transform (DHT)

DHT is a linear transform. In DHT N real numbers $x_0, x_1, \ldots, x_{N-1}$ are transformed in to N real numbers $H_0, H_1, \ldots, H_{N-1}$. The N-point DHT can be defined as follows:-

$$\begin{aligned} H_k &= \sum_{n=0}^{N-1} x_n \left[cos\left(\frac{2\pi nk}{N}\right) + sin\left(\frac{2\pi nk}{N}\right)\right] \\ &= \sum_{n=0}^{N-1} x(n).\ cas\left(\frac{2\pi nk}{N}\right) \end{aligned} \tag{20}$$

$$p_{m,n} = cas\left(\frac{2\pi mn}{N}\right) \tag{21}$$

Where $cas\theta = cos\theta + sin\theta$ and k=1, 2, 3… N-1.The DHT is also invertible transform which allows us to recover the x_n from H_k and inverse can be obtained by simply multiplying DHT of H_k by $\frac{1}{N}$.

3.4.3 Discrete Cosine Transform (DCT)

DCT matrix P of size N-by-N can be created by using equation (22)

$$D_{ij} = \begin{cases} \frac{1}{\sqrt{N}} & i = 0, \quad 0 \le j \le N-1 \\ \sqrt{\frac{2}{N}} cos \frac{\pi(2j+1)i}{2N} & 1 \le i \le N-1 \\ & 0 \le j \le N-1 \end{cases} \tag{22}$$

and DCT can be defined as:-

$$X_k = \sum_{n=0}^{N-1} x_n . cos\left[\frac{\pi}{N}\left(n+\frac{1}{2}\right)k\right] \qquad k=0, 1... N-1 \tag{23}$$

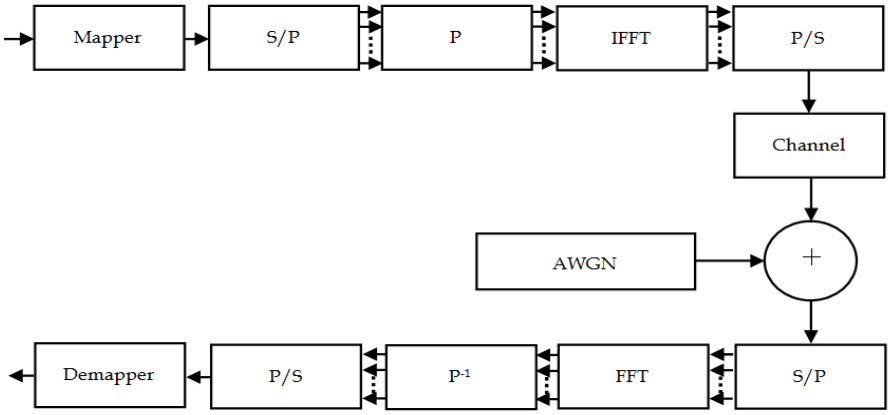

Fig. 9. Block diagram of OFDM system with Precording Techniques (Baig & Jeoti, 2010)

Fig.9 shows the precoding based OFDM system. In these system, the kernel of the WHT/DHT/DCT acts as a precoding matrix P of dimension $N= L\times L$ and it is applied to constellations symbols before the IFFT to reduce the correlation among the input sequence. In the precoding based systems baseband modulated data is passed through S/P converter which generates a complex vector of size L that can be written as $X=[X_0, X_1, \ldots, X_{L-1}]^T$ .Then precoding is applied to this complex vector which transforms this complex vector into new vector of length L that can be written as $Y=PX=[Y_0, Y_1, \ldots, Y_{L-1}]^T$, where P is a precoder matrix of size $N=L\times L$ and Y_m can be written as follows:-

$$Y_m = \sum_{l=0}^{L-1} p_{m,l} . X_l \qquad m = 0,1,... L-1 \tag{24}$$

$P_{m,l}$ means m^{th} row and l^{th} column of precoder matrix. Equation (24) represents the precoded constellations symbols. The complex baseband OFDM signal with N subcarriers can be written as:-

$$x_n = \frac{1}{\sqrt{N}} \sum_{m=0}^{N-1} Y_m . e^{j2\pi \frac{n}{N} m}, \qquad n = 0, 1, 2 \ldots N-1 \tag{25}$$

Table 1 summarizes the PAPR reduction techniques presented in the literature review. The clipping techniques have low implementation complexity but on the other hand, the clipping operation may introduce both in-band distortion and out-of-band radiation into the multicarrier signals, which degrades the OFDM system performance including BER and spectral efficiency. SLM and PTS both have high computational complexity. However, the

precoding based techniques show great promise as they are simple linear techniques to implement without any complex optimizations.

PAPR Reduction Technique	Implementation Complexity	Distortion	BER Degradation	Bandwidth Expansion	Power Increase	Data Rate Loss
Clipping & Filtering	LOW	YES	YES	NO	NO	NO
Selective Mapping	HIGH	NO	NO	YES	NO	NO
Partial Transmit Sequence	HIGH	NO	NO	YES	NO	YES
Precoding Based Techniques	LOW	NO	NO	NO	NO	NO

Table 1. Comparison of the PAPR Reduction Techniques

The main characteristics of precoding based techniques are, no bandwidth expansion, no power increase, no data rate loss, no BER degradation and distortionless.

4. Proposed PAPR reduction techniques

The random interleaved subcarrier mapping is favourable for the mobile WiMAX because it increases the capacity in the frequency selective fading channels and offers maximum frequency diversity. So, in this section, we present two precoding based random-interleaved OFDMA uplink systems for the PAPR reduction in the mobile WiMAX systems: Zadoff-Chu matrix transform (ZCMT) precoding based random-interleaved OFDMA uplink system and SLM based ZCMT precoded random-interleaved OFDMA uplink system. The PAPR of the proposed system is analyzed with root-raised-cosine (RRC) pulse shaping.

4.1 Zadoff-Chu sequences

Zadoff-Chu sequences are the class of polyphase sequences having optimum correlation properties. These sequences have an ideal periodic autocorrelation, constant magnitude and circular auto-orthogonality. The constant envelope feature of the Zadoff-Chu sequences can greatly alleviate the annoying peak-to-average power (PAPR) problem occurred in orthogonal frequency division multiplexing (OFDM) systems. According to (Chu, 1972; Popovic´, 1997), Zadoff-Chu sequences of length N can be defined as follows:-

$$z_n = \begin{cases} e^{\frac{j2\pi r}{N}\left(\frac{k^2}{2}+qk\right)} & for\ N\ Even \\ e^{\frac{j2\pi r}{N}\left(\frac{k(k+1)}{2}+qk\right)} & for\ N\ Odd \end{cases} . \tag{26}$$

Where k =0,1,2,…,N-1 , q is any integer, r is any integer relatively prime to N.

4.2 Autocorrelation property

Let us consider the periodic correlation property of Zadoff-Chu sequences with the same prime length. The periodic cross-correlation function can be defined as follows:-

$$\begin{aligned} \rho(m) &= \sum_{n=0}^{N-1} z_n z^*_{(n-m)modN} \\ &= \sum_{n=0}^{m-1} z_n z^*_{(n-m+N)} + \sum_{n=m}^{N-1} z_n z^*_{(n-m)} \end{aligned} \tag{27}$$

For the sake of simplicity we put q=0 and r=1 in equation (26), then using equation (26) in the above expression we get:-

$$\begin{aligned} &= \sum_{n=0}^{m-1} e^{\frac{[j\pi n^2]}{N}} . e^{\frac{[-j\pi(n-m+N)^2]}{N}} + \sum_{n=m}^{N-1} e^{\frac{[j\pi n^2]}{N}} . e^{\frac{[-j\pi(n-m)^2]}{N}} \\ &= \sum_{n=0}^{m-1} e^{\frac{[j\pi(2mn-2nN-m^2+2mN+N^2)]}{N}} + \sum_{n=m}^{N-1} e^{\frac{[j\pi(n^2-n^2-m^2+2mn)]}{N}} \\ &= \sum_{n=0}^{m-1} e^{\frac{[j\pi(2n-m+N)(m-N)]}{N}} + \sum_{n=m}^{N-1} e^{\frac{[j\pi(2mn-m^2)]}{N}} \end{aligned} \tag{28}$$

Note that,

$$\begin{aligned} e^{[\frac{j\pi(2n-m+N)(m-N)}{N}]} &= e^{[\frac{j\pi(2mn-2nN-m^2+2mN+N^2)}{N}]} \\ &= e^{[\frac{j\pi(2mn-m^2)}{N}]} . e^{[\frac{j\pi(2mN-2nN-N^2)}{N}]} \\ &= e^{[\frac{j\pi(2mn-m^2)}{N}]} . e^{j\pi(2m-2n-N)} \end{aligned} \tag{29}$$

While N is even 2m-2n-N is even. So, the equation (29) can be stated as: $\exp(\frac{j\pi(2mn-m^2)}{N})$.

Hence, we can combine two summations of equation (28) as follows:-

$$\begin{aligned} \rho(m) &= \sum_{n=0}^{N-1} e^{\frac{[j\pi(2mn-m^2)]}{N}} \\ &= e^{[\frac{-j\pi m^2}{N}]} . \sum_{n=0}^{N-1} e^{[\frac{j2\pi mn}{N}]} \end{aligned} \tag{30}$$

From equation (30), it is obvious that $\rho(m)$ =0, when m =0. Since, m and N are relatively prime to each other, $e^{[\frac{j2\pi m}{N}]}$ is a primitive N^{th} root of unity. Therefore, $e^{[\frac{j2\pi m}{N}]}$ is a N^{th} root of unity but not equal to 1 for the range of m {m:1,2,3,…,N} shown in equation (30). Hence, we can employ the theorem as follows:

$$\sum_{n=0}^{N-1} r^n = \begin{cases} N & r = 1 \\ 0 & r \neq 1 \end{cases} \tag{31}$$

where r is N^{th} root of unity, substituting equation (31) into equation (30), we get $|\rho(m)| = 0, \{m: 1,2,3,...,N\}$, At the end, it is concluded that the ideal periodic autocorrelation

property of Zadoff-Chu sequences makes it suitable candidate for PAPR reduction in OFDM systems.

4.3 Constant envelope property after IDFT

The Zadoff-Chu sequences have constant amplitude, and its IDFT has also constant amplitude. Additionally, zadoff-chu sequence is also Zadoff-Chu sequence after FFT or IFFT.

4.4 Orthogonality property

The DFT of the Zadoff-Chu sequences equal to the conjugate of the Zadoff-chu sequences as follows:-

$$\mathrm{DFT}(z_n) = (z_n)^* \tag{32}$$

Therefore, the orthogonality in time domain as well as in frequency domain is preserved.

4.5 Zadoff-Chu Matrix Transform (ZCMT)

Zadoff-Chu matrix transform (ZCMT) is used to lower the correlation relationship of the IFFT input sequence. The ZCMT precoding matrix must accomplish the following criteria:-

1. All the elements of the precoding matrix must have the identical magnitude.
2. The magnitude must be equal to: $\frac{1}{\sqrt{N}}$.
3. The ZCMT precoding matrix must be non-singular.

The first condition guarantees that each output symbol has the same quantity of information of every input data. The second requirement preserves the power at the precoder output. Finally, the third requirement ensures the recovery of the original data at the receiver. The kernel of the ZCMT is defined in equation (26). For $N = L \times L$ and $j = \sqrt{-1}$, the ZCMT kernel Z, of size $N = L \times L = L^2$ is obtained by reshaping the Zadoff-Chu sequence row-wise by $k = mL + l$, as hereunder:-

$$Z = \frac{1}{\sqrt{N}} \begin{bmatrix} z_{00} & z_{01} & \cdots & z_{0(L-1)} \\ z_{10} & z_{11} & \cdots & z_{1(L-1)} \\ \vdots & \vdots & \ddots & \vdots \\ z_{(L-1)0} & z_{(L-1)1} & \cdots & z_{(L-1)(L-1)} \end{bmatrix} \tag{33}$$

In other words, the L^2 point long Zadoff-Chu sequence fills the kernel of the matrix transform row-wise.

4.6 Proposed ZCMT precoding based random interleaved OFDMA system

Fig.10 shows a ZCMT precoding based random-interleaved OFDMA uplink system. In this system a precoding matrix Z of dimension $N = L \times L$ is applied to constellations symbols before the subcarrier mapping and IFFT to reduce the PAPR. In the ZCMT precoding based random-interleaved OFDMA systems, baseband modulated data is passed through S/P convertor which generates a complex vector of size M that can be written as follows:-

$$X = [X_0, X_1, X_2 \ldots X_{M-1}]^T \tag{34}$$

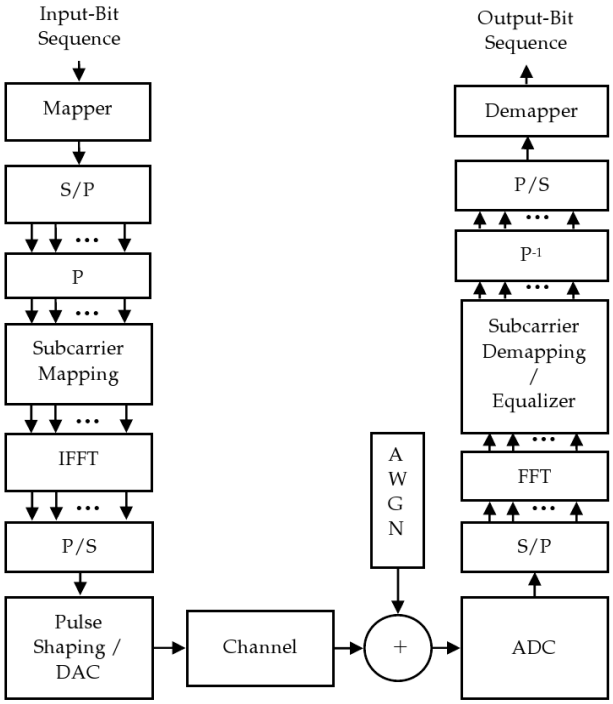

Fig. 10. ZCMT Precording based Random Interleaved OFDMA Uplink System

Then ZCMT precoding is applied to this complex vector which transforms this complex vector into new vector of same length L that can be written as follows:-

$$Y = ZX = [Y_0, Y_1, Y_2 \ldots Y_{M-1}]^T \tag{35}$$

where Z is a precoder matrix of size N=L×L and Y_m can be written as follows:-

$$Y_l = \sum_{m=0}^{L-1} z_{l,m}.X_m \qquad l = 0,1,\ldots L-1 \tag{36}$$

$z_{l,m}$ means l^{th} row of precoder matrix. Expanding equation (36), using row wise sequence reshaping $k = mL+l$ in equation (26) we get:-

$$\begin{aligned} Y_l &= \frac{1}{\sqrt{N}}\sum_{m=0}^{L-1}\left(e^{\frac{j2\pi r}{N}\left(\frac{(mL+l)^2}{2}+q(mL+l)\right)}\right).X_m = \frac{1}{\sqrt{N}}\sum_{m=0}^{L-1}\left(e^{\frac{j2\pi r}{N}\left(\frac{(m^2L^2+l^2+2mlL+2qmL+2lq)}{2}\right)}\right).X_m \\ &= \frac{1}{\sqrt{N}}\sum_{m=0}^{L-1}\left(e^{\frac{j\pi rm^2L^2}{N}}.e^{\frac{j\pi rl^2}{N}}.e^{\frac{j2\pi rmlL}{N}}.e^{\frac{j2\pi rqmL}{N}}.e^{\frac{j2\pi rlq}{N}}\right).X_m \end{aligned} \tag{37}$$

Since, N=L^2, then equation (37) can be reduced to

$$= \frac{1}{L}.e^{\frac{j\pi rl^2}{L^2}}.e^{\frac{j2\pi rlq}{L^2}}\sum_{m=0}^{L-1}\left(e^{\frac{j2\pi rlml}{L}}.\bar{X}_m\right) \tag{38}$$

where, $\bar{X}_m = (e^{\frac{j\pi rm^2}{L^2}}.e^{\frac{j2\pi rml}{L^2}}).X_m$, m=0,1,2,…,L-1, l =0,1,2,…,L-1. Equation (38) represents the ZCMT precoded constellations symbols. After precoding operation, the subcarrier mapping is performed on these ZCMT precoded constellations symbols in random-interleaved mode. After the subcarrier mapping in random interleaved mode, we get frequency domain samples $\{\hat{Y}_l : l = 0,1,2,...,N-1\}$. Mathematically, the subcarrier mapping in random interleaved mode can be done as follows:-

$$\hat{Y}_l = \begin{cases} Y_{\frac{l}{\hat{Q}}} & , l = \hat{Q}.k \quad 0 \le k \le M-1 \\ 0 & otherwise \end{cases} \tag{39}$$

Where $0 \le l \le N-1, N = Q.M, 0 \le \hat{Q} \le Q$, N: System subcarriers, M: User subcarriers (for one user), Q : Subchannels/Users (Q=N/L) . The k^{th} subcarrier of each group is assigned to the k^{th} user with index set: $\{(\gamma_{q,1}),(Q+\gamma_{q,2}),...,(L-1)Q+\gamma_{q,L-1})\}$, where $\{(\gamma_{q,1}),(\gamma_{q,2}),...,(\gamma_{q,L-1})\}$ are independent and identically distributed random variables with uniform distribution on (q=0,1,2,…,Q-1). Suppose the k^{th} user is assigned to subchannel k then the complex baseband ZCMT precoded random interleaved OFDMA signal for k^{th} user can be written as:-

$$x_n^{(k)} = \sum_{l=0}^{M-1} \hat{Y}_l^{(k)} . e^{j2\pi \frac{(lQ+\gamma_{q,k})}{N} n}, \quad n = 0,1...N-1 \tag{40}$$

where users index q =0,1,2,…,Q-1 and $\hat{Y}_l^{(k)}$ is modulated signal on subcarrier l for k^{th} user. The complex passband signal of ZCMT precoded random-interleaved OFDMA after RRC pulse shaping can be written as follows:-

$$x(t) = e^{j\omega_c t} \sum_{n=0}^{N-1} x_n^{(k)} . r(t - n\breve{T}) \tag{41}$$

where, ω_c is carrier frequency, $r(t)$ is baseband pulse, $\breve{T} = (\frac{M}{N}).T$. is compressed symbol duration after IFFT and T is symbol duration is seconds. The PAPR of the ZCMT precoded random-interleaved OFDMA signal in equation (41) with pulse shaping can be written as follows:-

$$PAPR(dB) = 10log_{10} \frac{\max(|x(t)|^2)}{E\{\max(|x(t)|^2)\}} \tag{42}$$

$E\{.\}$, denote expected value. If the amplitude of all subcarriers are normalized, $E\{max(|x(t)|^2)\} = N$, the equation (42) reduced to:-

$$PAPR(dB) = 10log_{10} \frac{\max(|x(t)|^2)}{N} \tag{43}$$

It should be pointed out that the orthogonality of the symbols after introducing precoding is maintained, as the precoding matrix is cyclic auto-orthogonal (Tasi et al., 2006). The instantaneous power of $x(t)$ can be defined as follows:-

$$p(t) = |x(t)|^2 = x(t) * x^*(t) \tag{44}$$

$$= \frac{1}{N}\sum_{i}^{N-1}\sum_{k}^{N-1} x_{zi}x_{zk}^{*}e^{\{j2\pi(i-k)t\}}$$

$$= \frac{1}{N}[N + 2Re\{\sum_{i}^{N-2}\sum_{k=i+1}^{N-1} x_{zi}x_{zk}^{*}e^{\{j2\pi(i-k)t\}}\}] \tag{45}$$

$$= 1 + \frac{2}{N}Re\{\sum_{m=1}^{N-1} e^{(j2\pi t)}\sum_{i=0}^{N-1-m} x_{zi}x_{z(i+m)}^{*}\}$$

For any complex c,

$$Re(c) \le |c|, \left|\sum c_n\right| \le \left|\sum c_n\right| .$$

That's why,

$$p(t) \le 1 + \frac{2}{N}\sum_{m=1}^{N-1}|\rho(m)| \tag{46}$$

where,

$$\rho(m) = \sum_{i=0}^{N-1-m} x_{zi}x_{z(i+m)}^{*} \text{ , } m = 0,1,2,\ldots,N\text{-}1$$

is the aperiodic autocorrelation function. It is concluded from equation (46) that if the aperiodic autocorrelation mold of the IFFT input sequence x_z is small ($\rho(m)$ for ≥1) then, the peak-power factor of the signal obtained by passing through the OFDM multi-carrier system also can be small (Tellambura, 1997).The peak value of the autocorrelation is the average-power of the input sequence. After that, if the number of subcarriers is not altered, this peak-value completely depends on the input sequence. It means that if the sidelobe of an autocorrelation function of an input sequence has greater value than other input sequences, the former has high correlation property. The IFFT operation can be expressed as multiplying sinusoidal functions to the input sequence, summing and sampling the results. Hence, the high correlation property of the IFFT input causes the sinusoidal functions to be arranged with in-phase form. After summing these in-phase functions, the output might have large peaks.

4.6.1 The effect of Zadoff-Chu Matrix Transform

To verify the contribution of ZCMT, we consider OFDMA system for QPSK modulation. Fig.11 shows that the aperiodic autocorrelation function of randomly generated QPSK sequence with the length 64 is given, which are normalized by the length. Thus the maximum value is 1 which is the average power of the sequence. It is obvious from the Fig.11 that two autocorrelation functions have different sidelobe value. If the sidelobes of autocorrelation have higher values, then the input sequence is highly correlated and its PAPR is high. The high correlation in the input to IFFT causes the subcarriers to align in-phase. After summing these in-phase functions, the output might have high amplitude resulting in higher PAPR. The sidelobe value of the proposed ZCMT is much smaller than the conventional OFDMA systems. Therefore, it is concluded that if we apply ZCMT precoder to the IFFT input sequence, it lower the correlation relationship of the OFDMA input sequence, thus PAPR can be reduced.

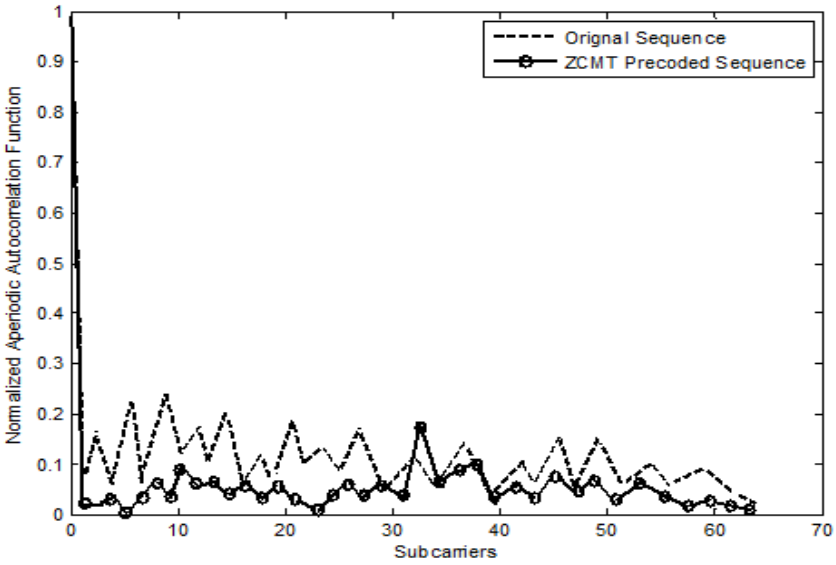

Fig. 11. The normalized autocorrelation function

4.7 Selective mapping to further improve ZCMT precoded random interleaved OFDMA system

Fig.12 shows the block diagram of the proposed SLM based ZCMT precoded random-interleaved OFDMA uplink system. Suppose data stream after S/P conversion is $X=[X_0,X_1,X_2,\ldots,X_{M-1}]^T$, and each data block is multiplied by V dissimilar phase sequences, each length equal to M, $B^{(v)}=[b_{v,0},b_{v,1},\ldots,b_{v,M-1}]^T$,$(v= 1, 2\ldots V)$, which results in the altered data blocks. Let us denote the altered data block for the v^{th} phase sequence is given by $X^{(v)}=[X_0b_{v,0},X_1b_{v,1},\ldots, X_{N-1}b_{v,M-1}]^T$, where $v=1,2,3,\ldots V$. Then, these altered data blocks are passed through the precoder, which transforms this complex vector into new vector of same length L that can be written as $Y=PX=[Y_0,Y_1,Y_2,\ldots, Y_{L-1}]^T$, where P is a ZCMT precoder matrix of size $N=L\times L$ and Y_m^v can be written as follows:-

$$Y_l^v = \sum_{m=0}^{M-1} z_{m,l} X_m^v \qquad l = 0,1,\ldots L-1 \tag{47}$$

where, $z_{m,l}$ means precoding matrix of m^{th} row and l^{th} column. Equation (47) represents the ZCMT precoded constellations signal. Then the subcarrier mapping of this precoded signal is done in random-interleaved mode. Suppose the k^{th} user is assigned to sub-channel k then the complex baseband SLM based ZCMT precoded OFDMA uplink signal for k^{th} user can be written as follows:-

$$x_n^{(k,v)} = \sum_{l=0}^{M-1} \hat{Y}_l^{(k,v)} . e^{j2\pi \frac{(lQ+\gamma_{q,k})}{N} n}, n = 0,1\ldots N-1 \tag{48}$$

$\hat{Y}_l^{(k,v)}$ is modulated signal on subcarrier m for k^{th} user.

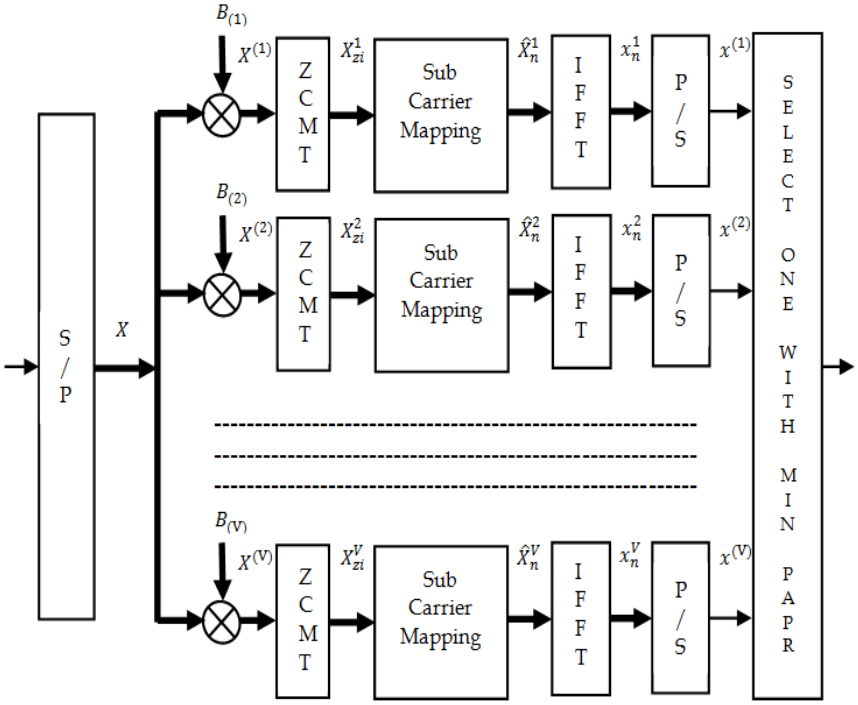

Fig. 12. Block diagram of SLM based ZCMT precoded random-interleaved OFDMA Uplink System

The precoding based SLM technique needs V (dissimilar phase sequences) IFFT operations and the information bits required as side information for each data block is $[\log_2 V]$. Precoding based SLM technique is applicable for any number of subcarriers and all types of modulation techniques. The PAPR reduction for precoding based SLM technique depends on the number of phase sequences V and the output data with lowest PAPR is selected by the transmitter for transmissions. The complex passband signal of random-interleaved OFDMA after RRC pulse shaping can be written as follows:-

$$x(t) = e^{j\omega_c t} \sum_{n=0}^{N-1} x_n^{(k,v)} . r(t - n\breve{T}) \tag{49}$$

where, ω_c is carrier frequency, $r(t)$ is baseband pulse, $\hat{T} = (\frac{M}{N}).T$ is compressed symbol duration after IFFT and T is symbol duration is seconds. The PAPR of the ZCMT precoded SLM based random-interleaved OFDMA uplink signal in (49) with RRC pulse shaping can be calculated by equation (43).

5. Simulation results

Extensive simulations in MATLAB(R) have been carried out to evaluate the performance of the proposed SLM based ZCMT precoded random-interleaved OFDMA uplink system with pulse shaping.

Channel Bandwidth	5MHz
Oversampling Factor	8
User Subcarriers	16
System Subcarriers	512
Precoding	WHT and ZCMT
Modulation	QPSK, 16-QAM, 64-QAM
Pulse Shaping	Root Raised Cosine (RRC)
Typical RRC Roll-Off Factor	$\alpha = 0.22$
Subcarrier Mapping Mode	Random Interleaved
CCDF Clip Rate	10^{-3}

Table 2. System Parameters

To show PAPR analysis of the proposed system, the data is generated randomly then modulated by QPSK, 16-QAM and 64-QAM respectively. We evaluate the PAPR statistically by using complementary cumulative distribution function (CCDF). The CCDF of the PAPR for ZCMT precoded random interleaved OFDMA uplink signal is used to express the probability of exceeding a given threshold $PAPR_0$ (CCDF = Prob (PAPR > $PAPR_0$)). We compared the simulation results of proposed system with WHT precoded random interleaved OFDMA uplink systems and conventional random interleaved OFDMA uplink systems. To show the PAPR analysis of proposed system with pulse shaping in MATLAB® we considered RRC rolloff factor $\alpha = 0.22$ with system subcarriers $N=512$ and user subcarriers $M=16$. All the simulations have been performed on 10^5 random data blocks. Simulation parameters that we use are given in the above Table 2.

Fig.13 shows CCDF comparison of PAPR for the ZCMT precoded random-interleaved OFDMA uplink system and the SLM based ZCMT precoded random-interleaved OFDMA uplink system with the WHT precoded random-interleaved OFDMA uplink systems and the conventional random-interleaved OFDMA uplink systems. At clip rate of 10^{-3}, with user subcarriers $M=16$ and system subcarriers $N=512$, the PAPR is 10 dB, 9.2 dB, 7.4 dB and 5.7 dB respectively, for the conventional random-interleaved OFDMA uplink systems, WHT precoded random-interleaved OFDMA uplink systems, ZCMT precoded random-interleaved OFDMA uplink systems and SLM based ZCMT precoded random-interleaved OFDMA uplink system respectively, using QPSK modulation.

Fig.14 shows CCDF comparison of PAPR for the ZCMT precoded random-interleaved OFDMA uplink system and the SLM based ZCMT precoded random-interleaved OFDMA uplink system with the WHT precoded random-interleaved OFDMA uplink systems and the conventional random-interleaved OFDMA uplink systems. At clip rate of 10^{-3}, with user subcarriers $M=16$ and system subcarriers $N=512$, the PAPR is 9.5 dB, 9.3 dB, 8.2 dB and 6.7

dB respectively, for the conventional random-interleaved OFDMA uplink systems, WHT precoded random-interleaved OFDMA uplink systems, ZCMT precoded random-interleaved OFDMA uplink systems and SLM based ZCMT precoded random-interleaved OFDMA uplink system respectively,, using 16-QAM modulation.

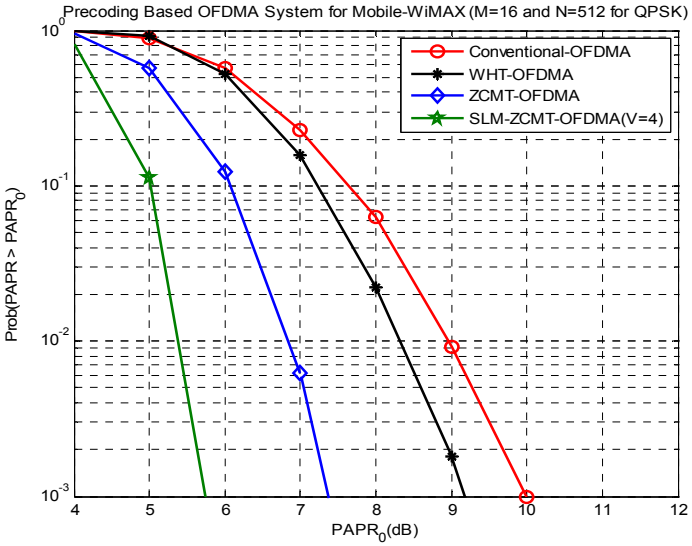

Fig. 13. CCDF Comparison of PAPR of the ZCMT precoded random-interleaved OFDMA uplink system and SLM based ZCMT precoded random-interleaved OFDMA uplink system with the WHT precoded random-interleaved OFDMA uplink system and the conventional random-interleaved OFDMA uplink system respectively, for QPSK modulation.

Fig.15 shows CCDF comparison of PAPR for the ZCMT precoded random-interleaved OFDMA uplink system and the SLM based ZCMT precoded random-interleaved OFDMA uplink system with the WHT precoded random-interleaved OFDMA uplink systems and the conventional random-interleaved OFDMA uplink systems. At clip rate of 10^{-3}, with user subcarriers M=16 and system subcarriers N=512, the PAPR is 9.8 dB, 9.6 dB, 8.7 dB and 6.7 dB respectively, for the conventional random-interleaved OFDMA uplink systems, WHT precoded random-interleaved OFDMA uplink systems, ZCMT precoded random-interleaved OFDMA uplink systems and SLM based ZCMT precoded random-interleaved OFDMA uplink system respectively, using 64-QAM modulation.

Fig.16 shows the SER performance of the ZCMT precoded random-interleaved OFDMA uplink systems; WHT precoded random-interleaved OFDMA uplink systems and the conventional random-interleaved OFDMA uplink systems respectively. The WiMAX Forum recommends using just two out of the six ITU models, which are Pedestrian B and Vehicular A (WiMAX, 2008). So, we use the ITU pedestrian B channel with additive white gaussian noise (AWGN) and MMSE equalization. The parameters for the ITU Pedestrian B channel model can be found in Table 3 (ITU, 1997).

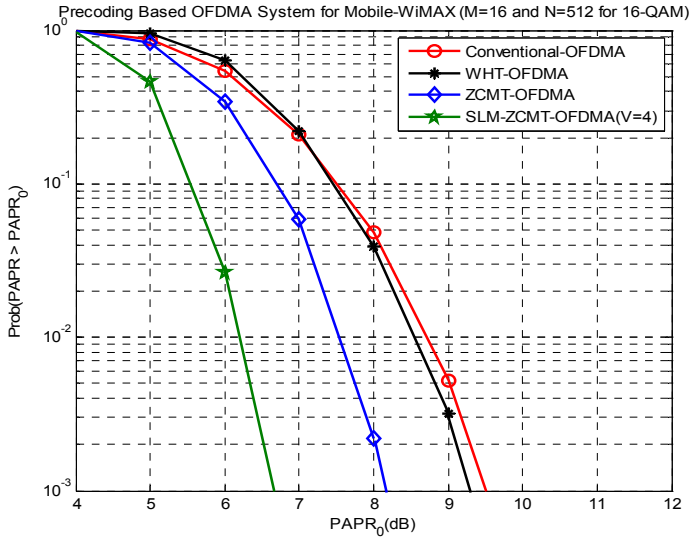

Fig. 14. CCDF Comparison of PAPR of the ZCMT precoded-random interleaved OFDMA uplink system and SLM based ZCMT precoded random-interleaved OFDMA uplink system with the WHT precoded random-interleaved OFDMA uplink system and the conventional random-interleaved OFDMA uplink system respectively, for 16-QAM modulation.

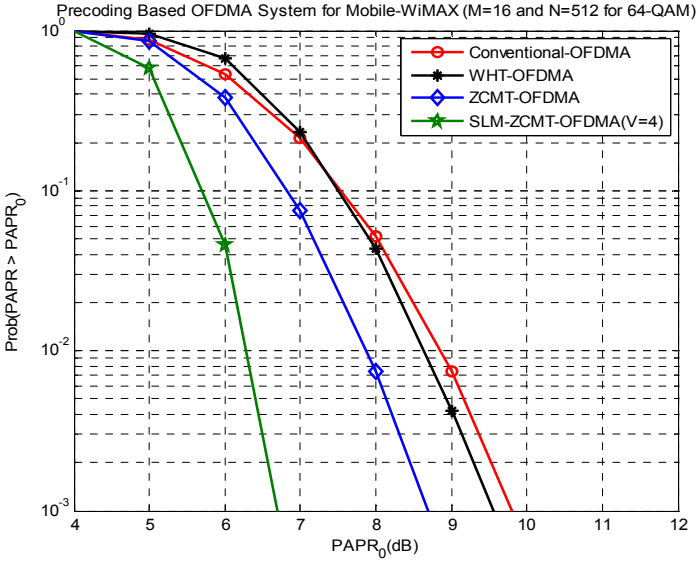

Fig. 15. CCDF Comparison of PAPR of the ZCMT precoded random-interleaved OFDMA uplink system and SLM based ZCMT precoded random-interleaved OFDMA uplink system with the WHT precoded random-interleaved OFDMA uplink system and the conventional random-interleaved OFDMA uplink system respectively, for 64-QAM modulation.

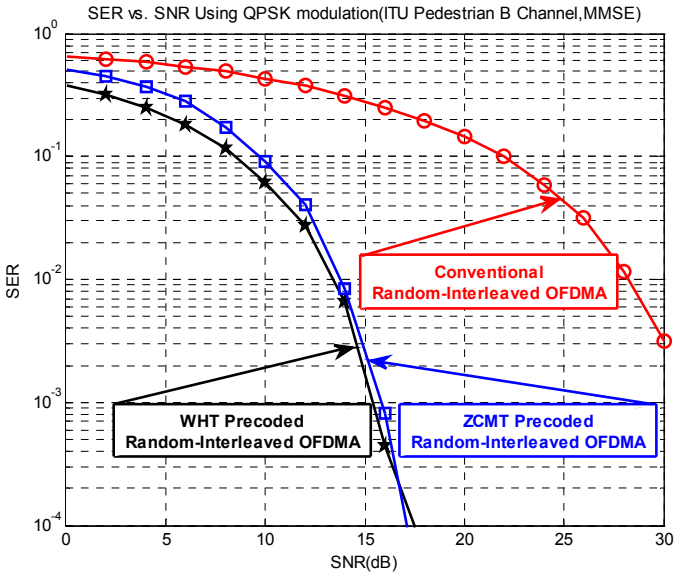

Fig. 16. SER vs. SNR Comparison of the ZCMT precoded Random-Interleaved OFDMA uplink system, the WHT precoded Random- Interleaved OFDMA uplink system and the conventional Random-Interleaved OFDMA uplink system, for sub-band 0 with QPSK modulation.

It is concluded from Fig.16 that the ZCMT precoded random-interleaved OFDMA uplink systems provides approximately same performance as that of the WHT precoded random-interleaved OFDMA systems but a significant SER performance improvement is seen over the conventional random interleaved OFDMA uplink systems for the sub-band 0 using QPSK modulation.

Table 4 summarizes the PAPR of random-interleaved OFDMA uplink systems, WHT random-interleaved OFDMA uplink systems, ZCMT precoded random-interleaved OFDMA uplink systems and SLM based ZCMT precoded random-interleaved OFDMA uplink systems respectively, using QPSK, 16-QAM and 64-QAM. Table 4 concludes that, the ZCMT precoded random-interleaved OFDMA uplink system and the SLM based ZCMT precoded random-interleaved OFDMA uplink system has lower PAPR than the WHT precoded random-interleaved OFDMA uplink systems and conventional random-interleaved OFDMA uplink systems.

Tap No.		**1**	**2**	**3**	**4**	**5**	**6**
ITU Pedestrian B Channel	**Relative Delay (ns)**	0	200	800	1200	2300	3700
	Average Power (dB)	0.0	-0.9	-4.9	-8.0	-7.8	-23.9
	Doppler Spectrum	Classic	Classic	Classic	Classic	Classic	Classic

Table 3. ITU Pedestrian B channel Parameters

Transmission Scheme	PAPR		
	QPSK	16-QAM	64-QAM
Conventional Random-Interleaved OFDMA	10 dB	9.5 dB	9.8 dB
WHT Random-Interleaved OFDMA	9.2 dB	9.3 dB	9.6 dB
ZCMT Random-Interleaved OFDMA	7.4 dB	8.2 dB	8.7 dB
SLM-ZCMT Random-Interleaved OFDMA	5.7 dB	6.7 dB	6.7 dB

Table 4. At CCDF of 10^{-3}, The PAPR Comparisons of the Conventional Random-Interleaved OFDMA uplink, WHT Random-Interleaved OFDMA uplink, ZCMT Random-Interleaved OFDMA uplink and SLM based ZCMT Random-Interleaved OFDMA uplink respectively, for users subcarriers (M=16) and system subcarriers (N=512)

6. Conclusion

In this chapter, we present a brief overview of the mobile WiMAX and typical PAPR reduction techniques available in the literature. We also introduce two precoding based systems: ZCMT precoded random-interleaved OFDMA uplink system and SLM based ZCMT precoded random-interleaved OFDMA uplink system, for PAPR reduction in mobile WiMAX systems. Computer simulation shows that the PAPR of the both proposed systems have less PAPR than the WHT precoded random-interleaved OFDMA uplink systems and conventional random-interleaved OFDMA uplink systems. These systems are efficient, signal independent, distortionless and do not require any complex optimizations. Additionally, these systems also take the advantage of the frequency variations of the communication channel and can also offer substantial performance gain in fading multipath channels. Thus, it is concluded that the both proposed uplink systems are more favourable than the WHT precoded random-interleaved OFDMA uplink systems and conventional random-interleaved OFDMA uplink systems for the mobile WiMAX systems.

7. References

Baig, I. & Jeoti, V. (2010). DCT Precoded SLM Technique for PAPR Reduction in OFDM Systems," *The 3rd International Conference on Intelligent and Advanced Systems, Kuala Lumpur, Malaysia*, 2010.

Baig, I. & Jeoti, V. (2010). Novel Precoding Based PAPR Reduction Techniques for Localized-OFDMA Uplink System of LTE-Advanced. *Journal of Telecommunication, Electronic and Computer Engineering (JTEC) Malaysia*, vol.2 no.1, pp 49-58, 2010.

Baig, I. & Jeoti, V. (2010). PAPR Analysis of DHT-Precoded OFDM System for M-QAM. *The 3rd International Conference on Intelligent and Advanced Systems,* Kuala Lumpur, Malaysia, 2010.

Baig, I. & Jeoti, V. (2010). PAPR Reduction in OFDM Systems: Zadoff-Chu Matrix Transform Based Pre/Post-Coding Techniques. *2nd International Conference on Computational Intelligence, Communication Systems and Networks, Liverpool, UK,* 2010.

Cho, Y. S.; Kim, J.; Yang, W. Y. & Kang, C. G. (2011). MIMO-OFDM Wireless Communications with Matlab. John Wiley & Sons, Inc. (Asia) Pte Ltd. ISBN:978-0-470-82561-7.

Chu, D.C. (1972). Polyphase codes with good periodic correlation properties. *IEEE Trans. Inform. Theory*, vol. IT-18, pp. 531-532, 1972.

Cimini, L. J. & Sollenberger, N. R. (2000). Peak-to-Average Power Ratio Reduction of an OFDM Signal Using Partial Transmit Sequences. *IEEE Commun. Lett.*, vol. 4, no. 3, pp. 86–88, Mar. 2000.

Han, S. H. & Lee, J. H. (2004). PAPR Reduction of OFDM Signals Using a Reduced Complexity PTS Technique. *Signal Processing Letters, IEEE*, vol.11, issue.11, pp: 887-890, 2004.

Han, S. H. & Lee, J. H. (2005). An overview of peak-to-average power Ratio reduction a techniques for multicarrier transmission. IEEE Wireless communication, vol.12, issue.2, pp: 56-65, 2005.

ITU, Document. (1997). Rec. ITU-R M.1225-Guidelines for Evaluation of Radio Transmission Technologies for IMT-2000, ITU-R, 1997.

Jayalath, A. & Tellambura, C. (2000). Adaptive PTS Approach for Reduction of Peak-to-Average Power Ratio of OFDM Signal," *Elect. Lett.*, vol. 36, no. 14, pp. 1226–28, July 2000.

Jeoti, V. & Baig, I. (2009). A Novel Zadoff-Chu Precoder Based SLM Technique for PAPR Reduction in OFDM Systems. invited paper, *Proceedings of 2009 IEEE International Conference on Antennas, Propagation and Systems*, Johor, Malaysia, 2009.

Jiang, T.; Yao, W.; Guo, P.; Song, Y. & Qu, D. (2006). Two novel nonlinear Companding schemes with iterative receiver to reduce PAPR in multicarrier modulation systems. *IEEE Trans. Broadcasting*, vol. 52, no. 2, pp. 268–273, 2006.

Knopp, R. & Humblet, P. A. (1995). Information Capacity and Power Control in Single-Cell Multiuser Communications. *IEEE Int. Conf. Communication*, pp. 331-335, 1995.

Kou, Y.; Lu, W. & Antoniou, A. (2007). A new peak-to- average power-ratio reduction algorithm for OFDM systems via constellation extension. *IEEE Trans. Wireless Communications*, vol. 6, no. 5, pp. 1823–1832, 2007.

Li, X. & Cimini, L.J. (1998) Effects of clipping and filtering on the performance of OFDM. IEEE Commun. Letter, 2(20), 131–133, 1998.

Lim, D. W.; No, J. S.; Lim, C. W. & Chung, H.(2005). A new SLM OFDM scheme with low complexity for PAPR reduction. *IEEE Signal Processing Letters*, vol. 12, no. 2, pp. 93–96, 2005.

Min, Y. K. & Jeoti, V. (2007). A Novel Signal Independent Technique for PAPR Reduction in OFDM Systems. *IEEE-ICSCN*, pp. 308-311, 2007.

Mourelo, J. T.(1999). Peak to Average Power Ratio Reduction for Multicarrier Modulation. *PhD thesis, University of Stanford, Stanford*, 1999.

Müller, S. H. & Huber, J. B. (1997). A Novel Peak Power Reduction Scheme for OFDM," *Proc. IEEE PIMRC '97*, Helsinki, Finland, pp. 1090–94, Sept. 1997.

Nee, V. & Wild, A. (1998) Reducing the peak-to-average power ratio of OFDM. IEEE VTC'98, vol.3, pp. 18–21, May 1998.

Nikookar, H. & Lidsheim, K. S. (2002). Random phase updating algorithm for OFDM transmission with low PAPR. *IEEE Trans. Broadcasting*, vol. 48, no. 2, pp. 123–128, 2002.

Popovic´, B. M. (1997). Spreading sequences for multi-carrier CDMA systems. *in IEE Colloquium CDMA Techniques and Applications for Third Generation Mobile Systems, London*, pp. 8/1–8/6, 1997.

Slimane, S. B. (2007). Reducing the peak-to-average power ratio of OFDM signals through precoding. *IEEE Trans. Vehicular Technology*, vol.56, no. 2, pp. 686–695, Mar. 2007.

Tasi, Y.; Zhang, G. & Wang, X. (2006). Orthogonal Polyphase Codes for Constant Envelope OFDM-CDMA System. *IEEE, WCNC*, pp.1396 – 1401, 2006.

Tellambura, C. (1997). Upper bound on peak factor of N-multiple carriers. Electronics Letters, vol.33, pp.1608-1609, Sept.1997.

Tellambura, C. (2001). Improved Phase Factor Computation for the PAR Reduction of an OFDM Signal Using PTS. *IEEE Commun. Lett.*, vol. 5, no. 4, pp. 135–37, Apr. 2001.

Thompson, S. C.; Ahmed, A. U.; Proakis, J. G.; Zeidler, J. R. & Geile, M. J. (2008).Constant envelope OFDM. *IEEE Trans. Communications*, vol. 56, pp. 1300-1312, 2008.

Tse, D. (1997). Optimal Power Allocation over Parallel Gaussian Broadcast Channels. *Proceedings of International Symposium on Information, Ulm Germany*, pp. 27, 1997.

Wang, H. & Chen, B. (2004). Asymptotic distributions and peak power analysis for uplink OFDMA signals. *in Proc. IEEE Acoustics, Speech, and Signal Processing Conference*, vol.4, pp.1085-1088, 2004.

Wang, L. & Tellambura, C. (2005). A Simplified Clipping and Filtering Technique for PAR Reduction in OFDM Systems. *Signal Processing Letters, IEEE*, vol.12, no.6, pp. 453-456, 2005.

WiMAX, Forum. (2008). WiMAX System Evaluation Methodology. Version 2.1, July 2008.

Yoo, S.; Yoon, S.; Kim, S.Y. & Song, I. (2006). A novel PAPR reduction scheme for OFDM systems: Selective mapping of partial tones (SMOPT). *IEEE Trans. Consumer Electronics*, vol. 52, no. 1, pp.40–43, 2006.

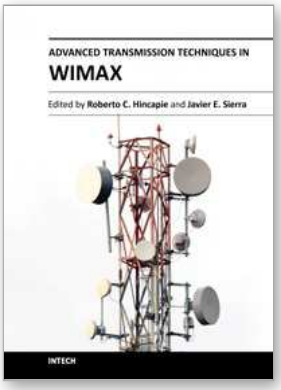

Advanced Transmission Techniques in WiMAX

Edited by Dr. Roberto Hincapie

ISBN 978-953-307-965-3
Hard cover, 336 pages
Publisher InTech
Published online 18, January, 2012
Published in print edition January, 2012

This book has been prepared to present the state of the art on WiMAX Technology. The focus of the book is the physical layer, and it collects the contributions of many important researchers around the world. So many different works on WiMAX show the great worldwide importance of WiMAX as a wireless broadband access technology. This book is intended for readers interested in the transmission process under WiMAX. All chapters include both theoretical and technical information, which provides an in-depth review of the most recent advances in the field, for engineers and researchers, and other readers interested in WiMAX.

InTech Europe
University Campus STeP Ri
Slavka Krautzeka 83/A
51000 Rijeka, Croatia
Phone: +385 (51) 770 447
Fax: +385 (51) 686 166
www.intechopen.com

InTech China
Unit 405, Office Block, Hotel Equatorial Shanghai
No.65, Yan An Road (West), Shanghai, 200040, China
中国上海市延安西路65号上海国际贵都大饭店办公楼405单元
Phone: +86-21-62489820
Fax: +86-21-62489821